

A Methodology to Relate Black Carbon Particle Number and Mass Emissions from Various Combustion Sources

Roger Teoh¹, Marc Stettler¹, Arnab Majumdar¹ & Ulrich Schumann²

¹ Centre for Transport Studies, Department of Civil and Environmental Engineering, Imperial College London, London, UK

² Deutsches Zentrum für Luft- und Raumfahrt, Institute of Atmospheric Physics, 82234 Oberpfaffenhofen, Germany

2018 Cambridge Particle Meeting
15th June 2018

Outline

1. Introduction & Motivation
2. Derivation of a new BC_N or EI_n Predictive Model
3. Model Validation
4. Uncertainty & Sensitivity Analysis
5. Conclusions & Further Work



Outline

1. Introduction & Motivation

2. Derivation of a new BC_N or EI_n Predictive Model

3. Model Validation

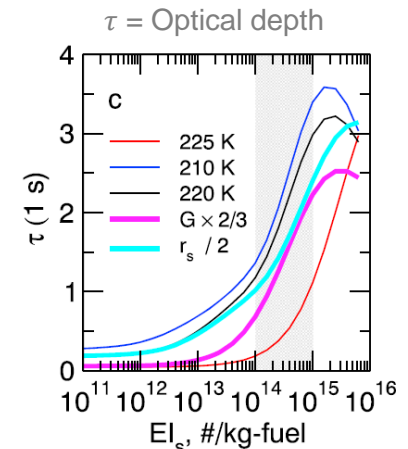
4. Uncertainty & Sensitivity Analysis

5. Conclusions & Further Work



Why is BC PN Emissions Important?

- Health Effects: Ultrafine particles have a higher probability of being deposited into the respiratory system, and translocated towards the circulatory system and internal organs.
- Climate Effects: During cruise, Black Carbon (BC) Particle Number (PN) emissions from aircraft engines act as a condensation nuclei for contrail formation.
 - ❖ No. of contrail ice particles = No. of aircraft BC particle emissions per kg-fuel burnt (EI_n in kg^{-1})
 - ❖ Different young contrail characteristics influenced by BC EI_n .
- Existing BC EI_n models for aviation emission assumes that BC particle morphologies remain constant irrespective of engine thrust settings.
- BC mass measurements and estimates remain more commonly available than the number metric.



Research Objectives

- 1) Develop a new model to estimate BC particle number emissions from mass based on the theory of fractal aggregates.
- 2) Validate the new model using BC measurements from three different emission sources.
- 3) Perform an uncertainty and sensitivity analysis to understand the accuracy and uncertainty bounds of the newly developed model.

Outline

1. Introduction & Motivation

2. Derivation of a new BC_N or EI_n Predictive Model

3. Model Validation

4. Uncertainty & Sensitivity Analysis

5. Conclusions & Further Work

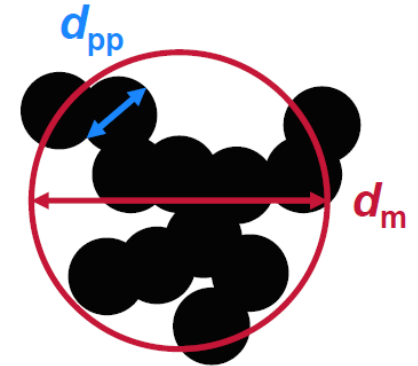


Development of a New BC PN Predictive Model

- Mass of one BC aggregate (m) is the summation of primary particle masses:

$$m = n_{pp} \rho_0 \left(\frac{\pi}{6} \right) d_{pp}^3$$

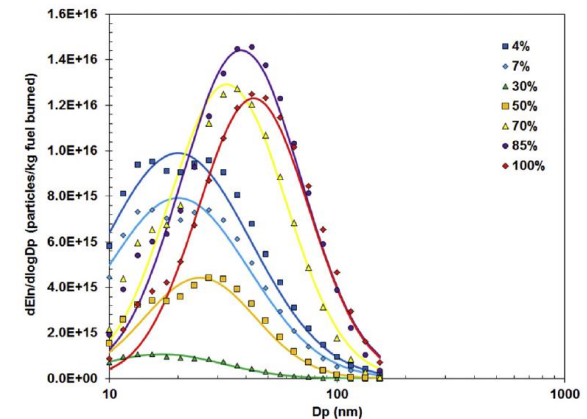
where n_{pp} = Number of primary particles in an aggregate
 ρ_0 = BC material density (1770 kg/m³)
 d_{pp} = Primary particle diameter



- The total mass of aggregates (M) is calculated using the integrated product of the aggregate mass and number weighted distribution:

$$M = \int_0^{\infty} m(d_m) n(d_m) d \ln d_m$$

where $n(d_m) = N \times p(d_m)$



Source: [11]

$$m = n_{pp} \rho_0 \left(\frac{\pi}{6}\right) d_{pp}^3$$

Development of a New BC PN Predictive Model

➤ In the free-molecular regime, the number of primary particles in an aggregate (n_{pp}) [6]:

$$n_{pp} = k_a \left(\frac{d_m}{d_{pp}}\right)^{2D_\alpha} \quad \text{or} \quad n_{pp} = \left(\frac{d_m}{d_{pp}}\right)^{D_{fm}}$$

where d_m = Aggregate mobility diameter

k_a = Scaling pre-factor

D_α = Projected area exponent

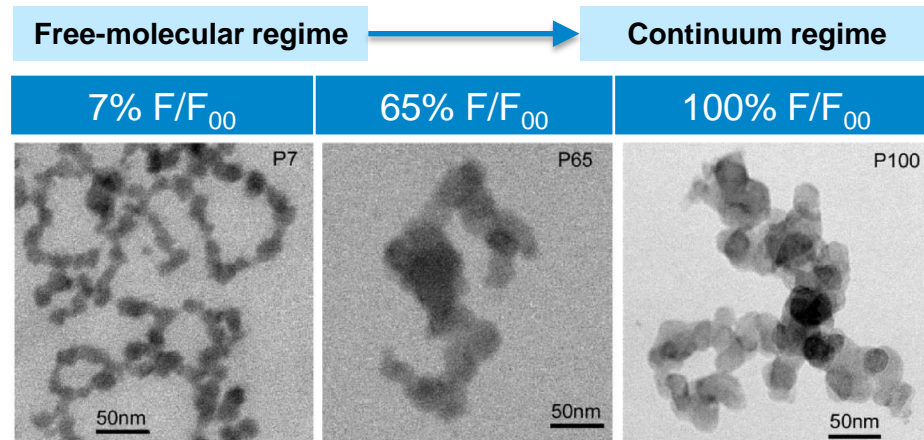
D_{fm} = Mass-mobility exponent

- Eggersdorfer et al. (2012) [7] suggested universal values of $k_a = 0.998$ and $D_\alpha = 1.069$ for aggregates formed of polydisperse primary particles, irrespective of the state of sintering.

➤ The Knudsen Number (Kn) is a dimensionless number equal to the ratio of the mean free path (λ) to the particle radius:

$$Kn = \frac{2\lambda}{d}$$

- Free-molecular regime: $Kn > 1$
- Continuum regime: $Kn \leq 1$
- Transition regime: $0.1 < Kn < 10$



$$m = n_{pp} \rho_0 \left(\frac{\pi}{6} \right) d_{pp}^3$$

Development of a New BC PN Predictive Model

- Relationship between primary particle (d_{pp}) and aggregate mobility diameter (d_m) [9]:

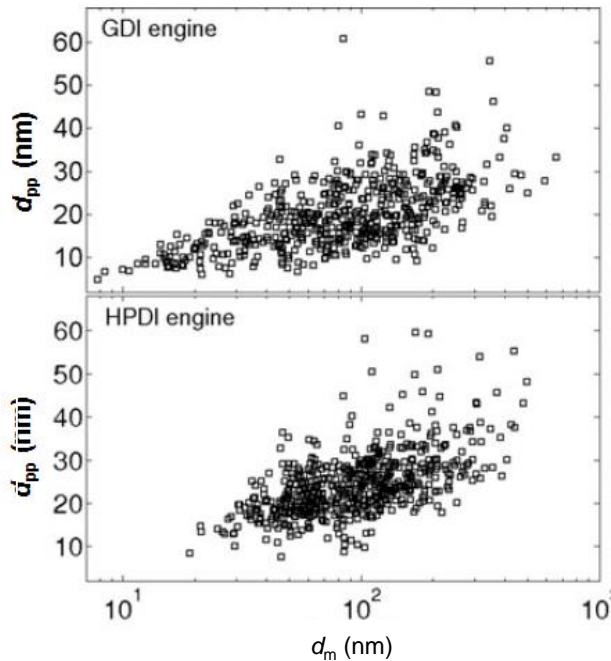
$$d_{pp} = k_{TEM} \times d_m^{D_{TEM}}$$

where prefactor-exponent coefficient pairs k_{TEM} & D_{TEM} are fitted with Transmission Electron Microscopy (TEM)

GDI engine:

$$k_{TEM} = 2.616 \times 10^{-6}$$

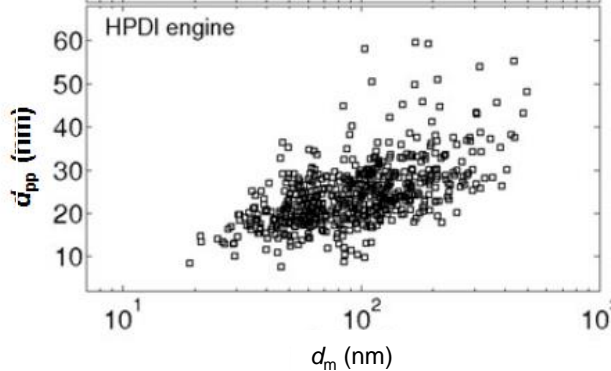
$$D_{TEM} = 0.30$$



HPDI engine:

$$k_{TEM} = 2.644 \times 10^{-6}$$

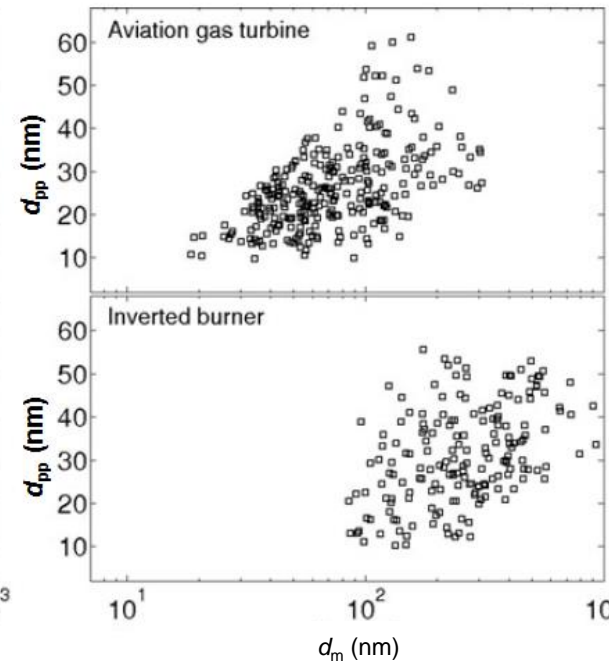
$$D_{TEM} = 0.29$$



Aviation gas turbine:

$$k_{TEM} = 1.621 \times 10^{-5}$$

$$D_{TEM} = 0.39$$



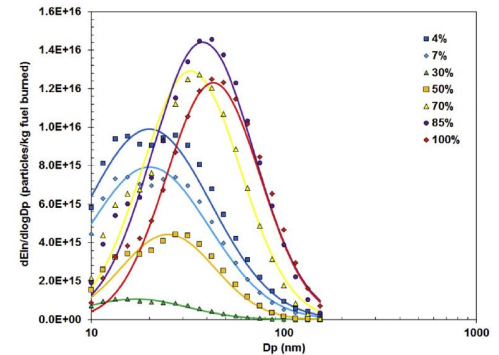
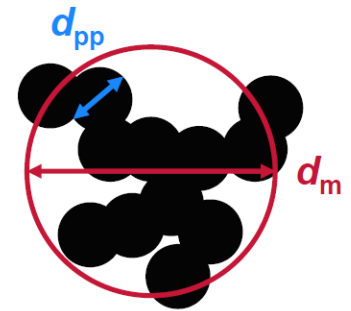
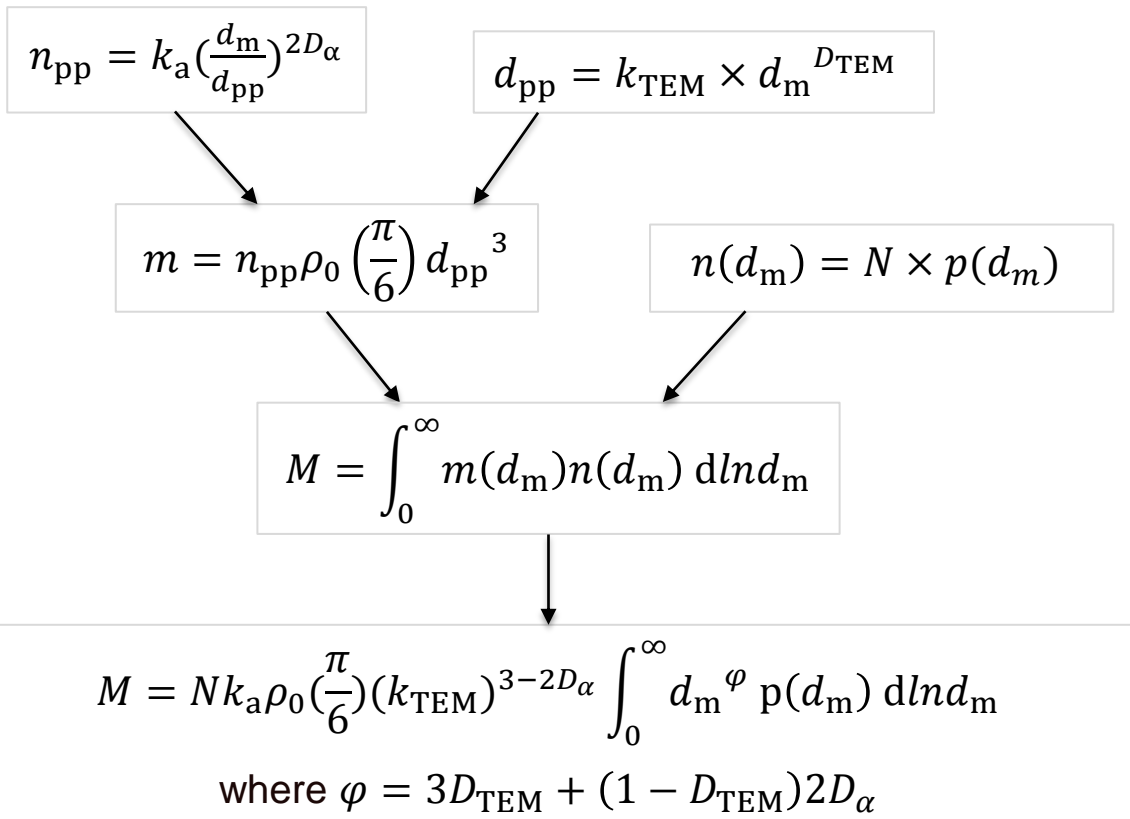
Inverted burner:

$$k_{TEM} = 2.465 \times 10^{-6}$$

$$D_{TEM} = 0.29$$

Development of a New BC PN Predictive Model

- The total mass of aggregates (M) for a given particle size distribution:



Source: [11]

Development of a new BC PN Predictive Model

- The remaining integral is the φ^{th} moment of a log-normal distribution:

$$M = N k_a \rho_0 \left(\frac{\pi}{6}\right) (k_{\text{TEM}})^{3-2D_\alpha} \text{GMD}^\varphi \exp\left(\frac{\varphi^2 \ln(\text{GSD})^2}{2}\right)$$

where GMD = Geometric Mean Diameter
 GSD = Geometric Standard Deviation

- Rearrange for N :

$$N = \frac{M}{k_a \rho_0 \left(\frac{\pi}{6}\right) (k_{\text{TEM}})^{3-2D_\alpha} \text{GMD}^\varphi \exp\left(\frac{\varphi^2 \ln(\text{GSD})^2}{2}\right)}$$



New N or EI_n Predictive Model, called the Fractal Aggregates (FA) Model.

- Advantages:

- ✓ New FA model relates BC mass, number and Particle Size Distribution (PSD) in one equation.
- ✓ Captures the change in particle morphology for different combustion conditions

Outline

1. Introduction & Motivation

2. Derivation of a new BC_N or EI_n Predictive Model

3. Model Validation

4. Uncertainty & Sensitivity Analysis

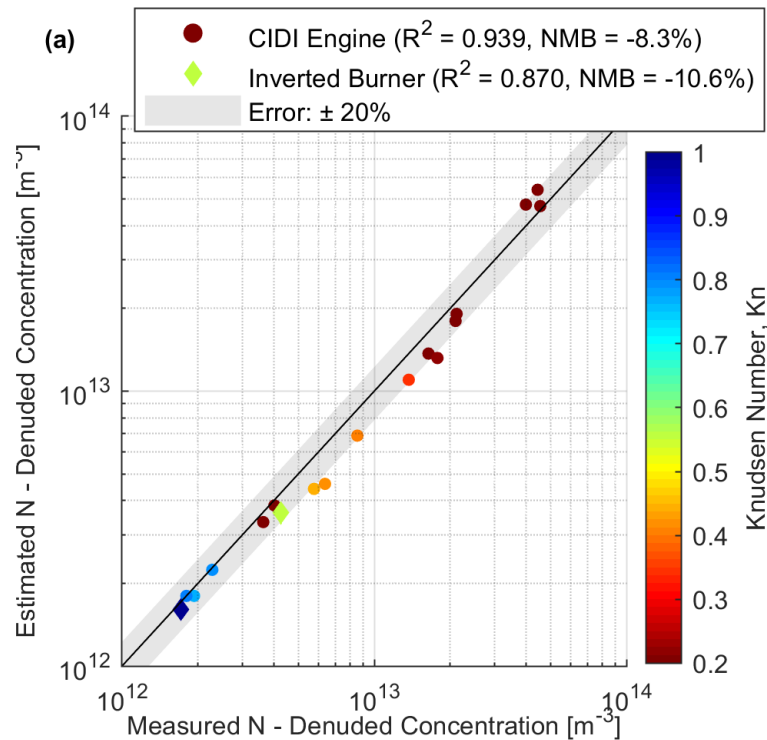
5. Conclusions & Further Work



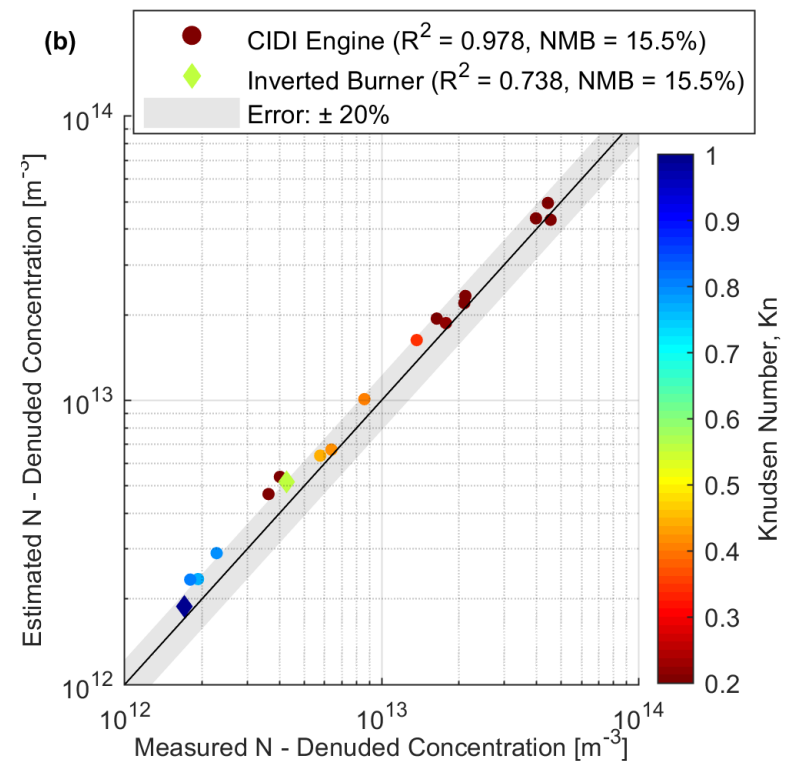
Model Validation – CIDI Engine & Inverted Burner

$$N = \frac{M}{k_a \rho_0 \left(\frac{\pi}{6}\right) (k_{TEM})^{3-2D_\alpha} \text{GMD}^\varphi \exp\left(\frac{\varphi^2 \ln(\text{GSD})^2}{2}\right)} \quad \text{where } \varphi = 3D_{TEM} + (1 - D_{TEM})2D_\alpha$$

(a) Experimentally fitted k_a and D_α values for each operating mode [14]



(b) Constant $k_a = 0.998$ and $D_\alpha = 1.069$ for all operating mode [7]

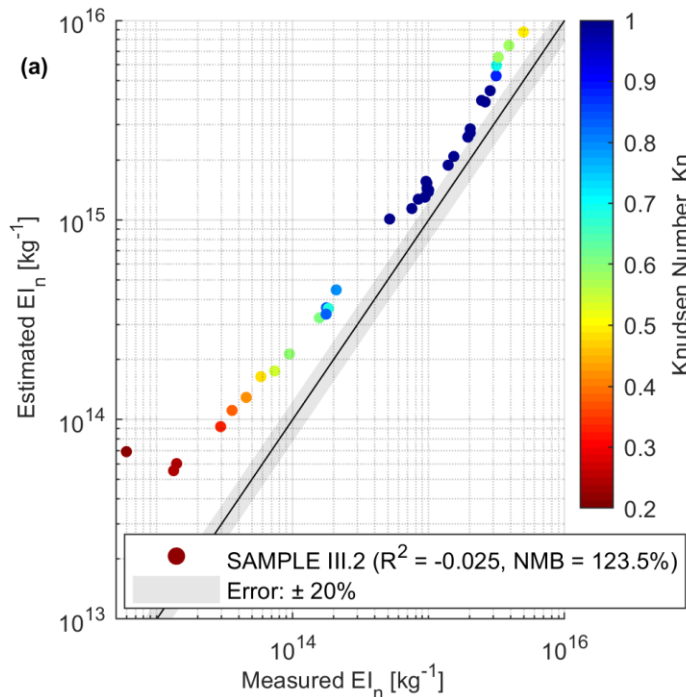


Model Validation – Aircraft Gas Turbine Engines

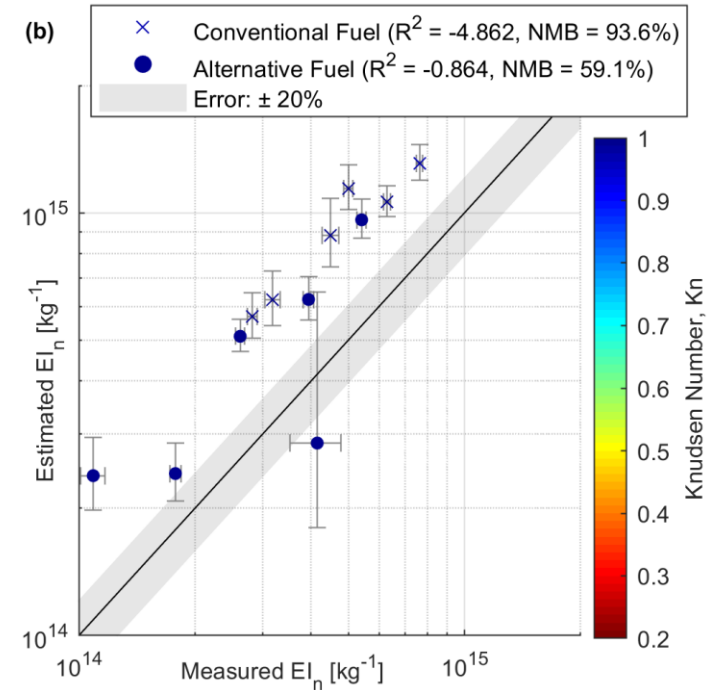
Constant $k_\alpha = 0.998$ and $D_\alpha = 1.069$ for all operating mode [7]

$$EI_n = \frac{EI_m}{k_a \rho_0 \left(\frac{\pi}{6}\right) (k_{TEM})^{3-2D_\alpha} GMD^\varphi \exp\left(\frac{\varphi^2 \ln(GSD)^2}{2}\right)} \quad \text{where } \varphi = 3D_{TEM} + (1 - D_{TEM})2D_\alpha$$

(a) Ground Validation



(b) Cruise Validation



➤ When k_α and D_α values of 0.998 and 1.069 [7] are applied to aircraft datasets, on average, we obtain negative R^2 and $> 100\%$ NMB values

Model Validation – Aircraft Gas Turbine Engines

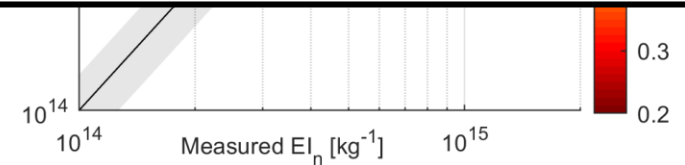
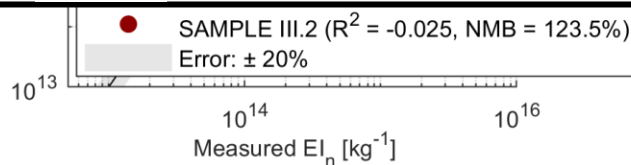
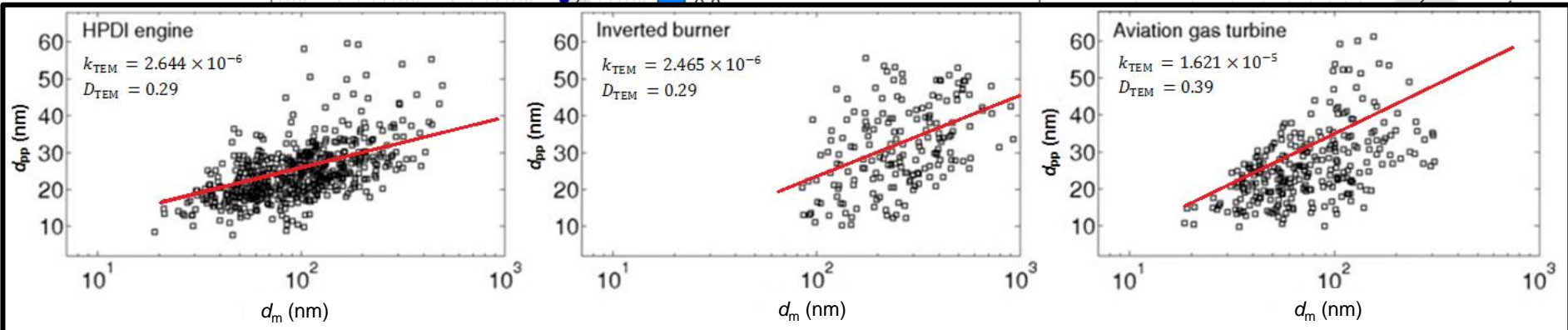
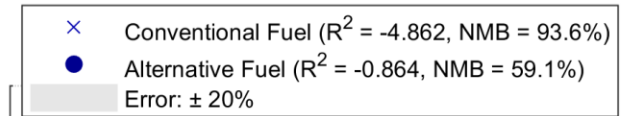
Constant $k_\alpha = 0.998$ and $D_\alpha = 1.069$ for all operating mode [7]

$$EI_n = \frac{EI_m}{k_a \rho_0 \left(\frac{\pi}{6}\right) (k_{TEM})^{3-2D_\alpha} GMD \varphi \exp\left(\frac{\varphi^2 \ln(GSD)^2}{2}\right)} \quad \text{where } \varphi = 3D_{TEM} + (1 - D_{TEM})2D_\alpha$$

(a) Ground Validation



(b) Cruise Validation



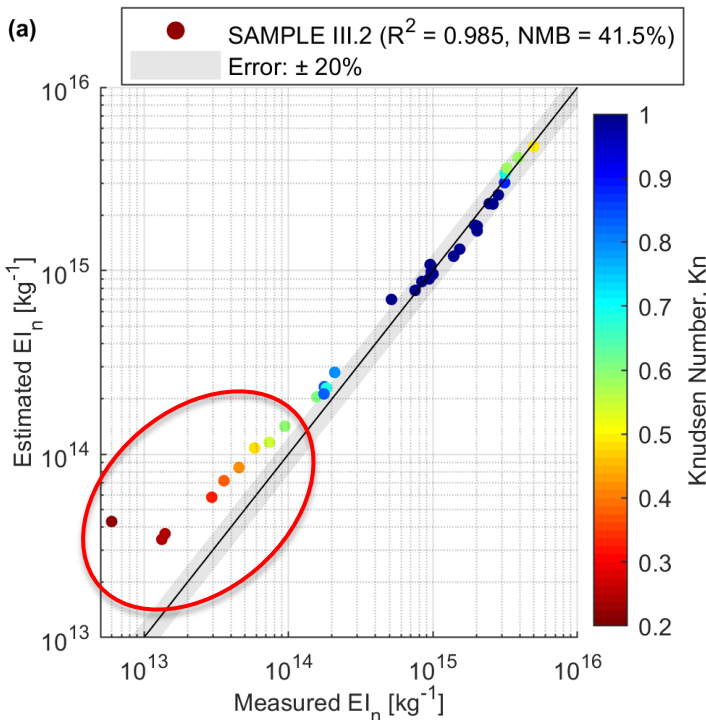
➤ When k_α and D_α values of 0.998 and 1.069 are applied to aircraft datasets, on average, we obtain negative R^2 and $> 100\%$ NMB values

Model Validation – Aircraft Gas Turbine Engines

$$EI_n = \frac{EI_m}{1 \times \rho_0 \left(\frac{\pi}{6}\right) (k_{TEM})^{3-D_{fm}} GMD^\varphi \exp\left(\frac{\varphi^2 \ln(GSD)^2}{2}\right)} \quad \text{where } \varphi = 3D_{TEM} + (1 - D_{TEM})D_{fm}$$

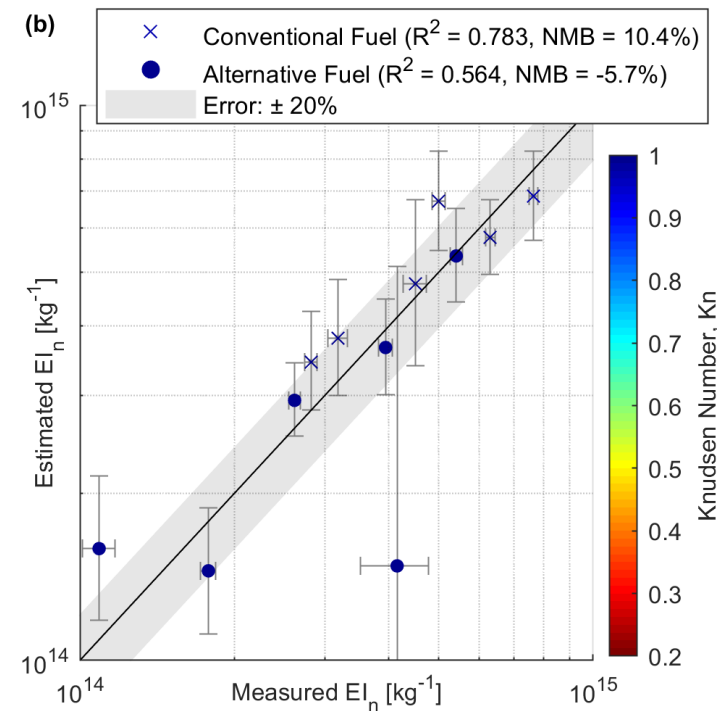
➤ Recall: $n_{pp} = k_a \left(\frac{d_m}{d_{pp}}\right)^{2D_\alpha}$ or $n_{pp} = \left(\frac{d_m}{d_{pp}}\right)^{D_{fm}}$. Hence, we assume that $k_a = 1$ and $D_\alpha = \frac{1}{2}D_{fm}$ [7]

(a) Ground Validation



Source: SAMPLE III.2 [10]

(b) Cruise Validation



Source: NASA ACCESS [15]

Outline

1. Introduction & Motivation

2. Derivation of a new BC_N or EI_n Predictive Model

3. Model Validation

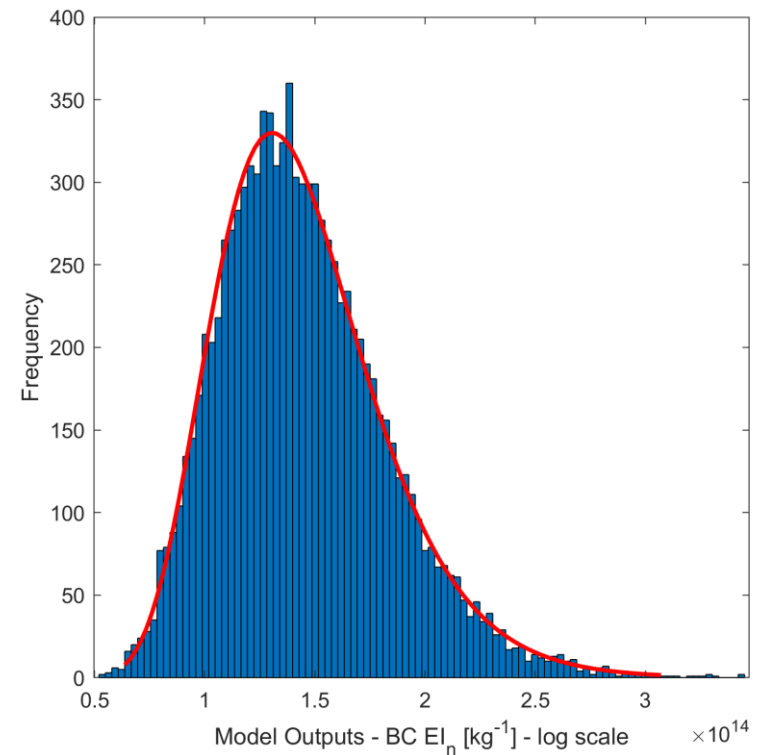
4. Uncertainty & Sensitivity Analysis

5. Conclusions & Future Work



Results: Uncertainty Analysis

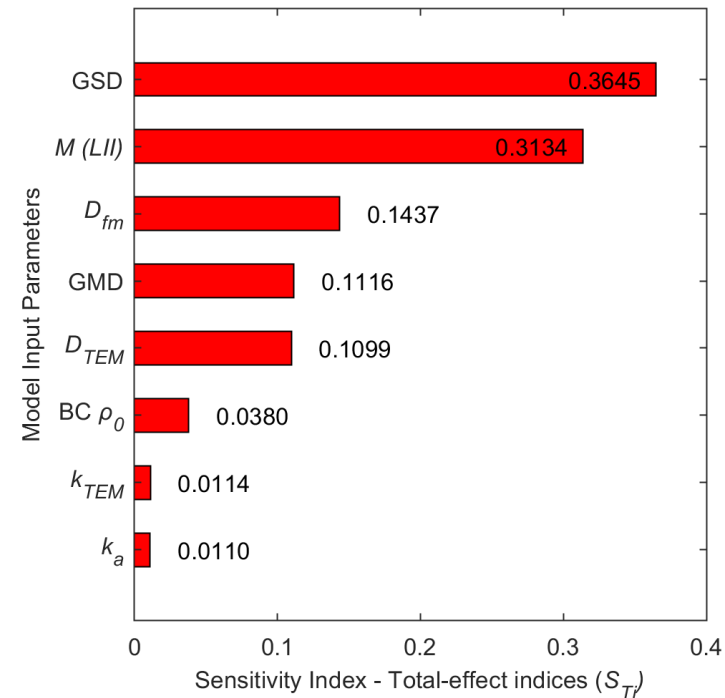
- Uncertainty analysis is performed using the Monte Carlo 1000-member ensembles [16].
- The uncertainty of the estimated EI_n are asymmetrically distributed (-37%, +55%) at 1.96σ .
- The asymmetrical distribution is due to the non-linearity of the FA model.
- An uncertainty analysis on the estimated EI_n was not conducted in previous aviation PN methodologies.



Results: Sensitivity Analysis

- A variance-based global sensitivity analysis identified that the uncertainties in GSD contribute to the largest sensitivity in the FA model output.
- A prioritisation can be recommended for future research to measure certain variables (such as M , D_{fm} , GMD and GSD) more accurately to reduce the uncertainty bounds of the FA model outputs.
- Given that k_a contributes to the lowest sensitivity to the estimated EI_n , the assumption of $k_a = 1$ across all engine types & F/F_{00} would not significantly affect the FA model outputs.

Sensitivity Analysis
(Measured Input Parameters)



Outline

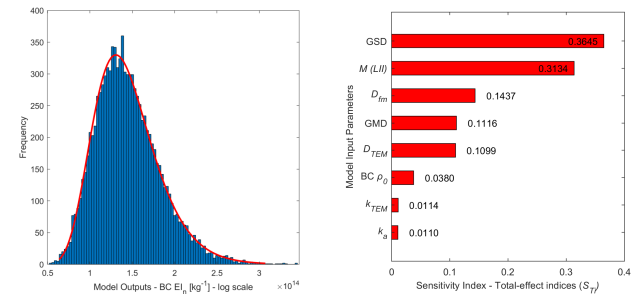
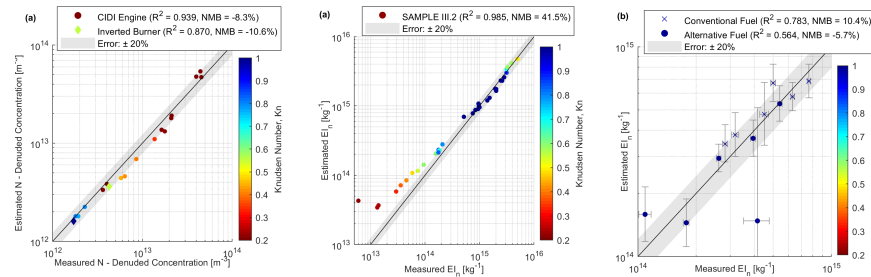
1. Introduction & Motivation
2. Derivation of a new BC_N or EI_n Predictive Model
3. Model Validation
4. Uncertainty & Sensitivity Analysis
5. Conclusions & Further Work



Conclusions

- A new methodology to relate BC Particle Number and Mass emissions is developed based on the theory of fractal aggregates.
- The new FA Model is validated with three different emission sources:
 - An internal combustion engine (CIDI)
 - An inverted burner
 - Two aircraft gas turbine engines
- An uncertainty analysis estimates N or EI_n to have an asymmetrical uncertainty bound (-36%, +54%) at 1.96σ .
- A sensitivity analysis shows that GSD is the most critical input parameter, followed by the M , D_{fm} and GMD.

$$N = \frac{M}{k_a \rho_0 \left(\frac{\pi}{6}\right) (k_{TEM})^{3-2D_\alpha} GMD \varphi \exp\left(\frac{\varphi^2 \ln(GSD)^2}{2}\right)}$$



Future Work

FA Model Application to Aviation Emissions:

Is there a net climate benefit in diverting flights to avoid contrail formation?

Aircraft Activity Dataset:
CARATS Open Data, Japan



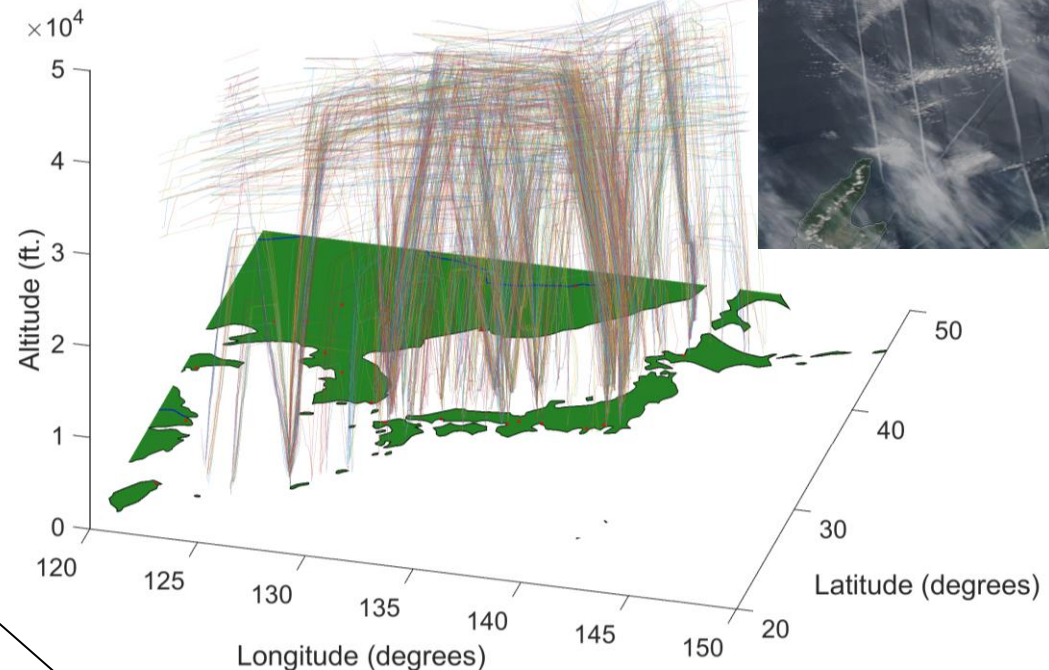
Emissions:
 CO_2 , BC EI_n (FA Model) & EI_m ,...

Ambient atmospheric conditions:
ECMWF Dataset

Contrail Model:
CoCiP

Climate
Impacts

Air Traffic
Management



Thank you, questions?

roger.teoh15@imperial.ac.uk

Research Postgraduate,
Centre for Transport Studies,
Department of Civil and Environmental Engineering
Imperial College London

Acknowledgements:

This PhD is funded by The Lloyds Register Foundation, and the Skempton Scholarship from the Department of Civil and Environmental Engineering, Imperial College London.

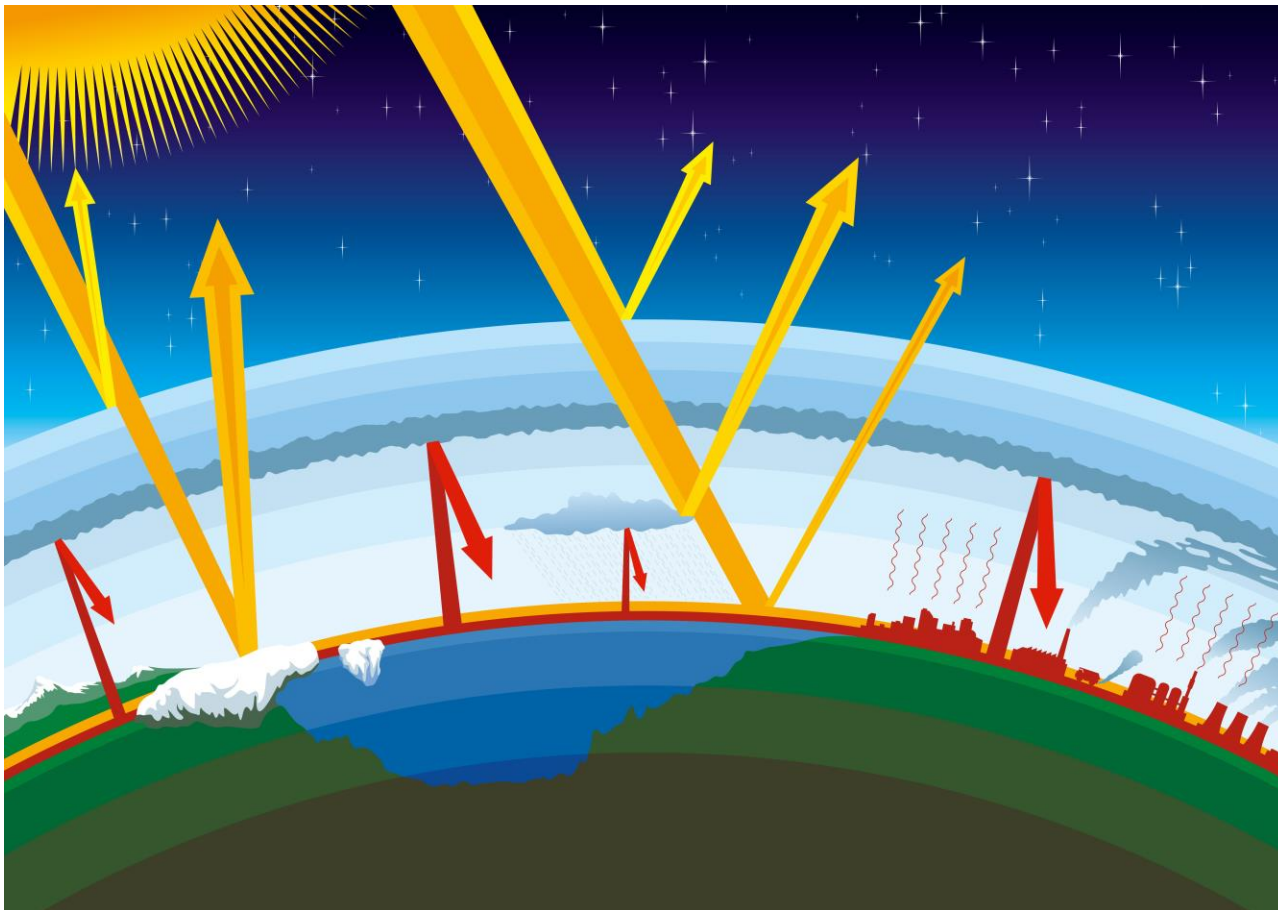
References

- [1] Kärcher, B. (2016) The importance of contrail ice formation for mitigating the climate impact of aviation. *Journal of Geophysical Research: Atmospheres*. 121 (7), 3497-3505.
- [2] Petzold, A., Döpelheuer, A., Brock, C. & Schröder, F. (1999) In situ observations and model calculations of black carbon emission by aircraft at cruise altitude. *Journal of Geophysical Research: Atmospheres*. 104 (D18), 22171-22181.
- [3] Döpelheuer, A. (2002) *Anwendungsorientierte Verfahren Zur Bestimmung Von CO, HC Und Ruß Aus Luftfahrttriebwerken*.
- [4] Barrett, S., Prather, M., Penner, J., Selkirk, H., Balasubramanian, S., Döpelheuer, A., Fleming, G., Gupta, M., Halthore, R. & Hileman, J. (2010) Guidance on the use of AEDT gridded aircraft emissions in atmospheric models. *US Federal Aviation Administration Office of Environment and Energy*.
- [5] Lee, D., Pitari, G., Grewe, V., Gierens, K., Penner, J., Petzold, A., Prather, M., Schumann, U., Bais, A. & Berntsen, T. (2010) Transport impacts on atmosphere and climate: Aviation. *Atmospheric Environment*. 44 (37), 4678-4734.
- [6] Sorensen, C.M., 2011. The mobility of fractal aggregates: a review. *Aerosol Science and Technology*, 45(7), pp.765-779
- [7] Eggersdorfer, M.L., Kadau, D., Herrmann, H.J. and Pratsinis, S.E., 2012. Aggregate morphology evolution by sintering: number and diameter of primary particles. *Journal of aerosol science*, 46, pp.7-19.
- [8] Liati, A., Brem, B.T., Durdina, L., Vöggtli, M., Arroyo Rojas Dasilva, Y., Dimopoulos Eggenschwiler, P. and Wang, J., 2014. Electron microscopic study of soot particulate matter emissions from aircraft turbine engines. *Environmental science & technology*, 48(18), pp.10975-10983.
- [9] Dastanpour, R. & Rogak, S. N. (2014) Observations of a correlation between primary particle and aggregate size for soot particles. *Aerosol Science and Technology*. 48 (10), 1043-1049.
- [10] Boies, A. M., Stettler, M. E., Swanson, J. J., Johnson, T. J., Olfert, J. S., Johnson, M., Eggersdorfer, M. L., Rindlisbacher, T., Wang, J. & Thomson, K. (2015) Particle emission characteristics of a gas turbine with a double annular combustor. *Aerosol Science and Technology*. 49 (9), 842-855.
- [11] Lobo, P., Hagen, D.E., Whitefield, P.D. and Raper, D., 2015. PM emissions measurements of in-service commercial aircraft engines during the Delta-Atlanta Hartsfield Study. *Atmospheric Environment*, 104, pp.237-245.

References

- [12] Graves, B., Olfert, J., Patychuk, B., Dastanpour, R. and Rogak, S., 2015. Characterization of particulate matter morphology and volatility from a compression-ignition natural-gas direct-injection engine. *Aerosol Science and Technology*, 49(8), pp.589-598.
- [13] Dastanpour, R., Momenimovahed, A., Thomson, K., Olfert, J. and Rogak, S., 2017. Variation of the optical properties of soot as a function of particle mass. *Carbon*, 124, pp.201-211.
- [14] Dastanpour, R., Rogak, S.N., Graves, B., Olfert, J., Eggersdorfer, M.L. and Boies, A.M., 2016. Improved sizing of soot primary particles using mass-mobility measurements. *Aerosol Science and Technology*, 50(2), pp.101-109.
- [15] Moore, R. H., Thornhill, K. L., Weinzierl, B., Sauer, D., D'Ascoli, E., Kim, J., Lichtenstern, M., Scheibe, M., Beaton, B. & Beyersdorf, A. J. (2017) Biofuel blending reduces particle emissions from aircraft engines at cruise conditions. *Nature*. 543 (7645), 411-415.
- [16] Saltelli, A., Ratto, M., Andres, T., Campolongo, F., Cariboni, J., Gatelli, D., Saisana, M. & Tarantola, S. (2008) *Global sensitivity analysis: the primer*. , John Wiley & Sons
- [17] Schumann, U., 2012. A contrail cirrus prediction model. *Geoscientific Model Development*, 5, pp.543-580.
- [18] Abegglen, M., Durdina, L., Brem, B. T., Wang, J., Rindlisbacher, T., Corbin, J. C., Lohmann, U. & Sierau, B. (2015) Effective density and mass-mobility exponents of particulate matter in aircraft turbine exhaust: Dependence on engine thrust and particle size. *Journal of Aerosol Science*. 88 135-147.

Global Warming



Source: http://globalwarming-facts.info/wp-content/uploads/shutterstock_91110830.jpg

Existing BC EI_n Models for Aviation Emissions

1) Average BC Particle Mass [2]

- ❖ Total BC mass divided by an average mass of each BC particle
- ❖ $BC EI_n = \frac{BC EI_m}{(3.2 \times 10^{-17})}$

2) EI_n/EI_m Ratio with Altitude Variations [3]

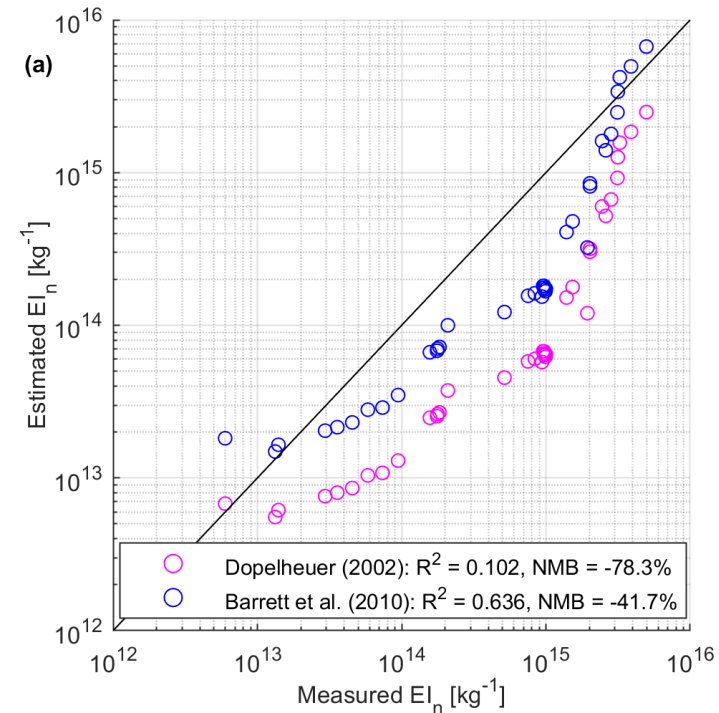
- ❖ $\approx 5 \times 10^{15}$ to 1.6×10^{16} particles per g(BC)
- ❖ Used in the Aero2K Global Aviation Emissions Inventories

3) Assumed Particle Diameter [4]

- ❖ $EI_n = \frac{EI_m}{\left(\frac{\pi}{6}\right) \rho_{NV} \times GMD^3 \times \exp\left(\frac{9}{2} (\ln GSD)^2\right)}$
- ❖ Assume log-normal distribution, GMD and GSD fixed at 38nm and 1.6 respectively.

4) BC EI_n Range [1]

- ❖ $BC EI_n \approx 10^{14}$ to 10^{15} per kg fuel burned



KEY LIMITATION:

Existing BC EI_n models do not include a dependence on the change in BC aggregate morphologies vs engine thrust settings

Knudsen Number, Kn

$$\text{Knudsen Number, } Kn = \frac{2\lambda}{d}$$

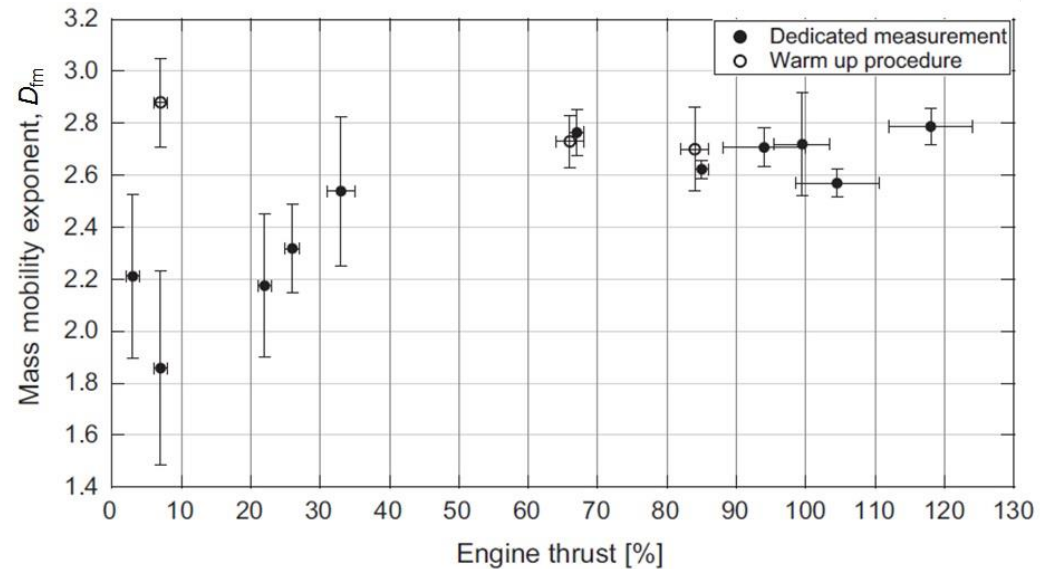
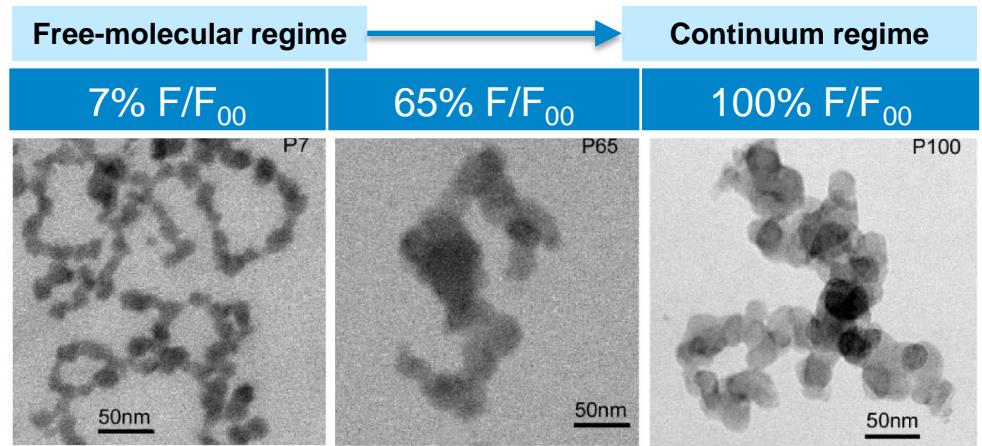
- Mean free path, λ = Average distance travelled by an aggregate between successive collisions with gas molecules.
- The mean free path of at a given pressure (P_1) can be estimated using standard atmospheric conditions (P_0, λ_0) as a reference:

$$\lambda_1 = \lambda_0 \frac{P_0}{P_1}, \quad \text{where} \quad P_0 = 1 \text{ atm} \ \& \ \lambda_0 = 0.066 \ \mu\text{m}$$

- For the emissions from an internal combustion engine and aircraft gas turbine, the pressure in the combustor is used for P_1
- For inverted burner emissions, we assume that $P_1 = 1 \text{ atm}$

Knudsen Number, Kn

- Free-molecular regime: $Kn > 1$
- Continuum regime: $Kn \leq 1$
- Transition regime: $0.1 < Kn < 10$



How is k_a and D_α Experimentally Fitted?

Dastanpour et al. (2016) [14]

METHOD 1: Estimation of k_a and D_α using Optimisation

- Combining equations $n_{pp} = k_a \left(\frac{d_m}{d_{pp}}\right)^{2D_\alpha}$ and $m = n_{pp} \left(\frac{\pi}{6}\right) d_{pp}^3 \rho_0$ to obtain:

$$d_{pp} = \left[\frac{k_a \pi \rho_0}{6m} (d_m)^{2D_\alpha} \right]^{\frac{1}{2D_\alpha - 3}}$$

- Optimum k_a and D_α values are calculated using regression to minimise the difference between the TEM determined d_{pp} and the above equation.

METHOD 2: Estimation of k_a and D_α using Experimental Measurements

- Combining equations $n_{pp} = k_a \left(\frac{d_m}{d_{pp}}\right)^{2D_\alpha}$ and $n_{pp} = \frac{m}{m_{pp}}$ to obtain:

$$\ln\left(\frac{m}{m_{pp}}\right) = 2D_\alpha \ln\left(\frac{d_m}{d_{pp}}\right) + \ln(k_a)$$

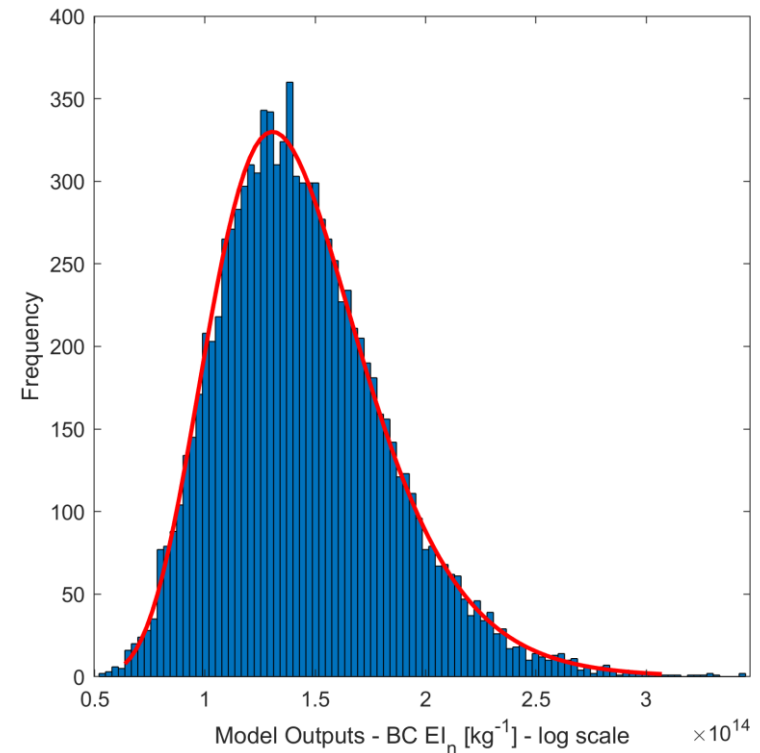
- Mass-mobility data (obtained from CPMA and DMA), and TEM-obtained d_{pp} and m_{pp} were used in the above equation to obtain k_a and D_α values.

Uncertainty & Sensitivity Analysis

$$EI_n = \frac{EI_m}{k_a \rho_0 \left(\frac{\pi}{6}\right) (k_{TEM})^{3-2D_\alpha} GMD^\varphi \exp\left(\frac{\varphi^2 \ln(GSD)^2}{2}\right)}$$

Variable	Fixed F/F ₀₀	Mean (μ)	Std Dev (σ)
BC EI _m (LII)	0.4	2.7 mg/kg	(25%/1.96)*μ
ρ ₀	0.4	1770 kg/m ³	70
k _a	0.4	1	(2.4%/1.96)*μ
D _{fm}	0.4	2.76	(7.9%/1.96)*μ
k _{TEM}	0.4	1.621x10 ⁻⁵	(7.2%/1.96)*μ
D _{TEM}	0.4	0.39	(7.9%/1.96)*μ
GMD	0.4	18.49 nm	(6.5%/1.96)*μ
GSD	0.4	1.73	(7.6%/1.96)*μ

- Uncertainty Distribution for all Parameters: Normal

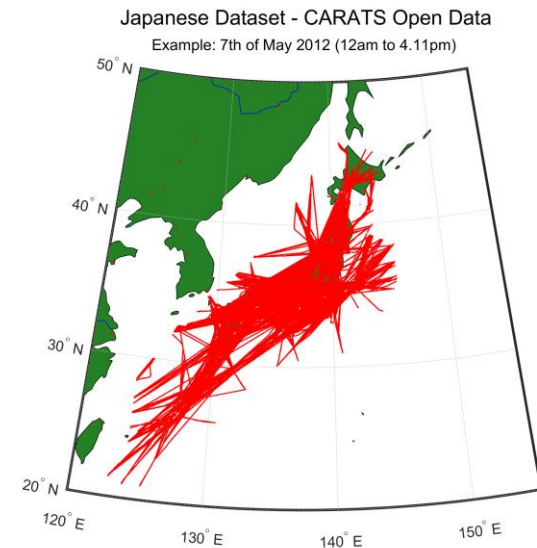


Model Application to Aviation Emissions

Can we apply the new FA model to estimate BC EI_n for global civil aviation, or at an individual flight level?

$$EI_n = \frac{EI_m}{\rho_0 \left(\frac{\pi}{6}\right) (k_{TEM})^{3-D_{fm}} GMD^\varphi \exp\left(\frac{\varphi^2 \ln(GSD)^2}{2}\right)}$$

where $\varphi = 3D_{TEM} + (1 - D_{TEM})D_{fm}$



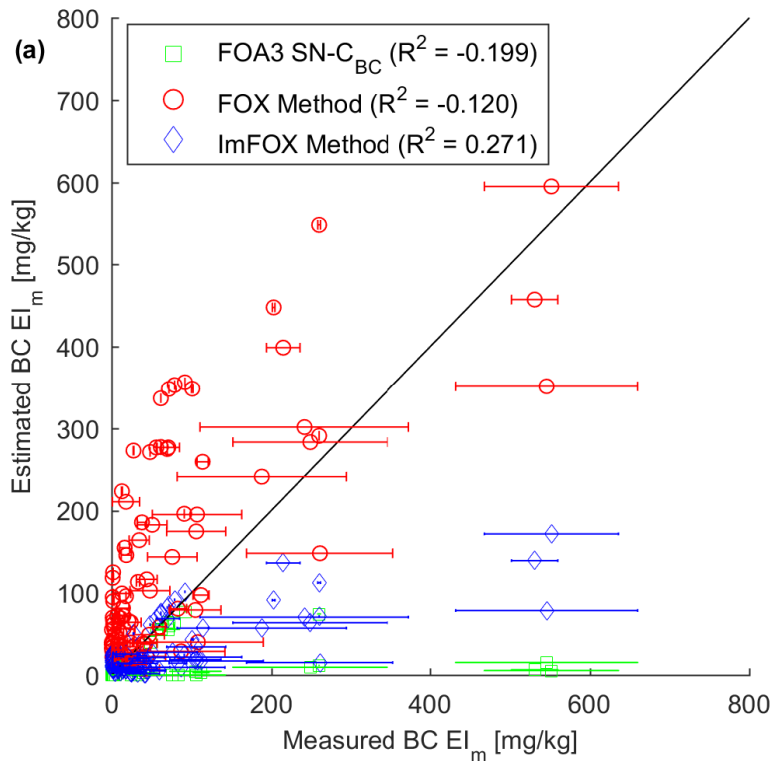
Requirements:

- Estimate different input variables (BC EI_m , GMD, GSD and D_{fm}) versus engine thrust settings (F/F_{00}).

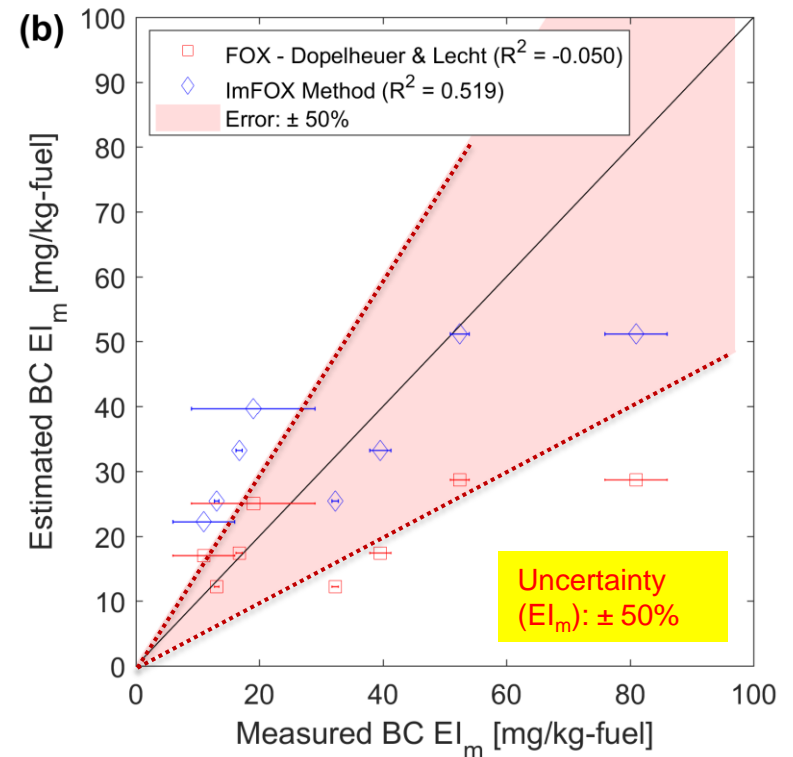
Model Inputs – (1) Existing BC EI_m Models

$$EI_n = \frac{EI_m}{\rho_0 \left(\frac{\pi}{6}\right) (1.621 \times 10^{-5})^{3-D_{fm}} GMD^\varphi \exp\left(\frac{\varphi^2 \ln(GSD)^2}{2}\right)}$$

(a) Ground Conditions



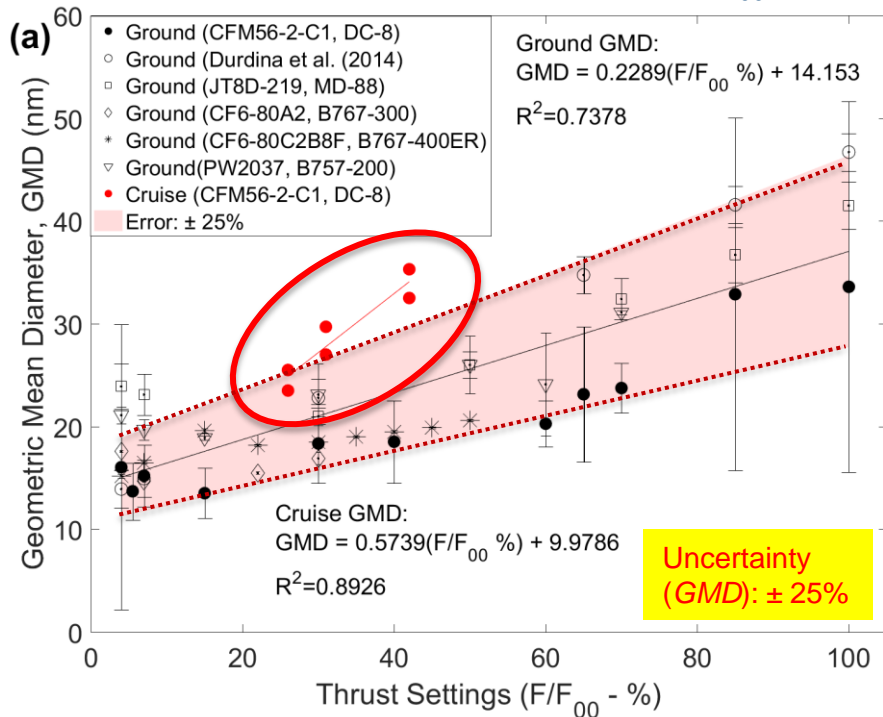
(b) Cruise Conditions



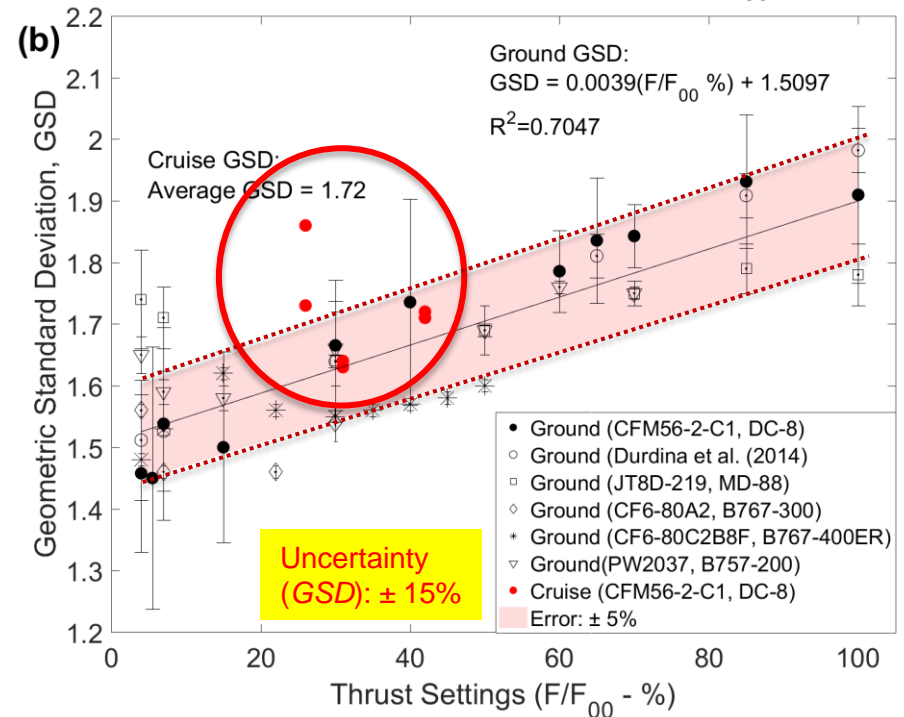
Model Inputs – (2) GMD & (3) GSD

$$EI_n = \frac{EI_m}{\rho_0 \left(\frac{\pi}{6}\right) (1.621 \times 10^{-5})^{3-D_{fm}} \mathbf{GMD}^\varphi \exp\left(\frac{\varphi^2 \ln(\mathbf{GSD})^2}{2}\right)}$$

(a) BC GMD vs. Thrust Settings (F/F_{00})



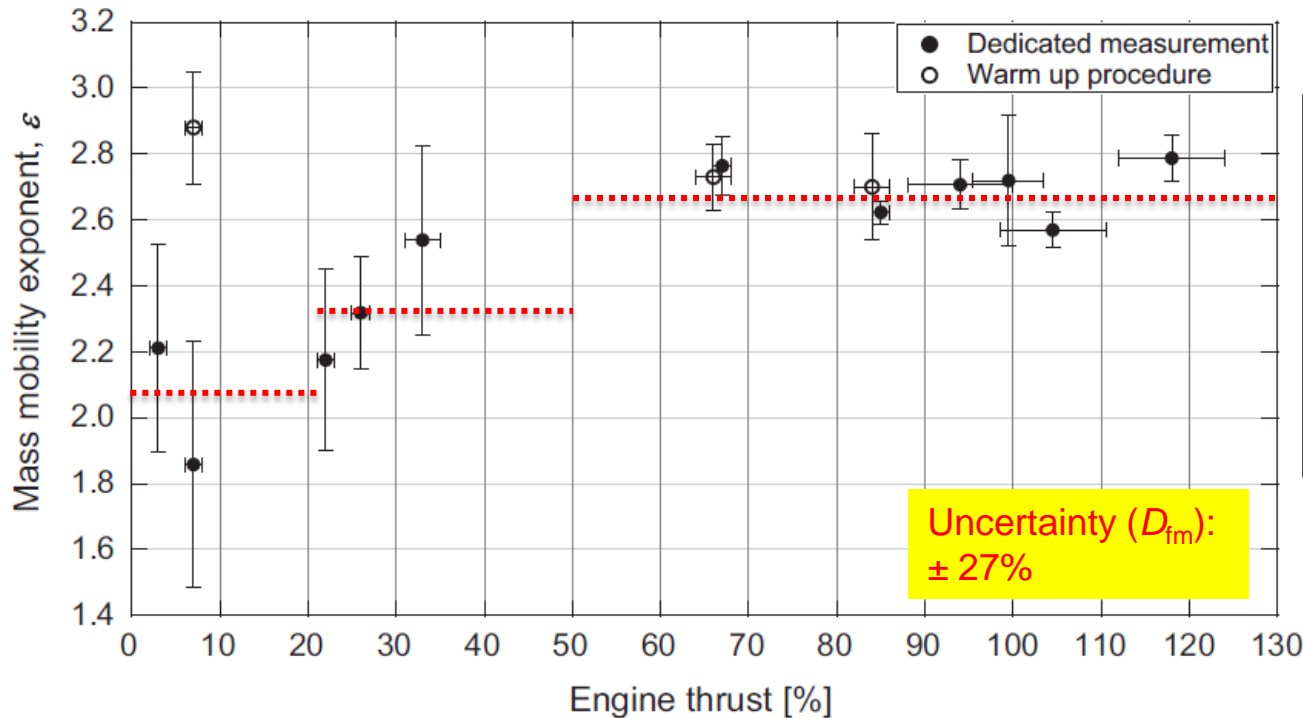
(b) BC GSD vs. Thrust Settings (F/F_{00})



Model Input Parameters – (4) D_{fm}

$$EI_n = \frac{EI_m}{\rho_0 \left(\frac{\pi}{6}\right) (1.621 \times 10^{-5})^{3-D_{fm}} GMD^\varphi \exp\left(\frac{\varphi^2 \ln(GSD)^2}{2}\right)}$$

where $\varphi = 1.17 + 0.61 D_{fm}$



$$D_{fm} = 2.04, \text{ for } 0.03 \leq \frac{F}{F_{00}} < 0.2$$

$$D_{fm} = 2.35, \text{ for } 0.2 \leq \frac{F}{F_{00}} < 0.50$$

$$D_{fm} = 2.64, \text{ for } 0.5 \leq \frac{F}{F_{00}} < 1$$

* D_{fm} values are for Singular Annular Combustor (SAC) turbofan engines only

Source: [19]

FA Model Validation – Estimated Inputs

- Cruise BC EI_n and EI_m measurements were available from the SULFUR experimental campaigns. [20] [21]
- No GMD, GSD and D_{fm} measurements were available.
- Estimated inputs for GMD, GSD and D_{fm} versus F/F_{00} (specified in previous slides) were used.
- Validation results justify the use of the GMD, GSD and D_{fm} predictive relations as model inputs to the FA model.

